

旋转磁场辅助激光加工微孔的机理及试验研究

王银飞, 朱浩, 张朝阳*, 张天帅, 吴予澄, 杜文武

江苏大学机械工程学院, 江苏 镇江 212013

摘要 为了改善激光钻孔的几何形貌,提高其刻蚀深度和减小微孔锥度,以 304 不锈钢为试验材料,采用旋转磁场辅助激光钻孔的加工工艺,研究了在不同转速旋转磁场下,微孔刻蚀深度、表面喷溅、孔壁几何形貌和内壁氧含量的变化,探索了在有/无旋转磁场作用下,单脉冲能量对微孔锥度的影响。试验结果表明,随着旋转磁场转速的提升,微孔刻蚀深度增加,表面喷溅更加显著,氧含量降低,但过快的转速会使孔壁几何形貌变差。此外,旋转磁场的引入可以有效减小微孔锥度,且单脉冲能量越大,微孔锥度降低得越明显。

关键词 激光技术; 激光钻孔; 旋转磁场; 形貌; 锥度; 刻蚀深度

中图分类号 TN249

文献标志码 A

DOI: 10.3788/CJL202249.1602001

1 引言

随着航空航天领域科学技术的发展,微孔的激光加工具有越来越重要的意义。与传统机械加工和电火花加工微孔等方法相比,激光打孔具有加工效率高、速度快、成本低和适用范围广等特点,且几乎不受材料限制,清洁无污染,可以实现数量多、密度高的群孔加工。

超短脉冲激光加工由于其较高的加工精度,已逐渐成为高质量微孔加工的首选。但现有的研究发现,超短脉冲激光加工依然存在重铸层、微裂纹和熔渣等缺陷,同时其效率远不如传统的长脉冲激光加工。采用磁场辅助激光钻孔,可以进一步减少超短脉冲激光加工产生的缺陷,例如改善激光钻孔形貌,增加刻蚀深度和减小微孔锥度。在磁场对微孔形貌及性能影响方面,Lu 等^[1]采用旋转电磁场辅助激光打孔,利用电磁场约束等离子体,试验表明,旋转电磁场可以使微孔表面飞溅物减少,重铸层变薄,内壁微裂纹减少。Chang 等^[2]利用旋转磁场辅助激光打孔,研究表明,旋转动态磁场可以改善入口圆度和降低热影响区。朱苏凯^[3]对超声-磁场耦合辅助激光打孔进行了研究,结果表明,外加磁场可改善孔壁质量。在磁场对微孔刻蚀深度及锥度影响方面,Ye 等^[4]对外加横向静态磁场辅助激光打孔进行了研究,发现微孔孔深增加,锥度减小。Balamurugan 等^[5]用 2.3×10^{-2} T 静态磁场辅助激光对 6061 铝进行了打孔研究,发现磁场辅助可以减小微孔锥度。李涛等^[6]利用静态磁场辅助脉冲激光旋切割孔,发现微孔入口直径减小,微孔锥度减小。

在激光钻孔过程中,激光加工材料产生的等离子体对激光束具有屏蔽作用,导致微孔形貌质量差,刻蚀效率低,锥度大。施加磁场(MF)可以对等离子体形成约束,致使等离子体沿磁场方向膨胀,即在水平方向扩散,从而减弱对激光的屏蔽作用^[7]。为了改善激光钻孔形貌,增加刻蚀深度和减小微孔锥度,可采用旋转磁场(RMF)辅助激光钻孔的方法。旋转磁场产生的洛伦兹力使得等离子体中的带电粒子作加速运动,这会对熔融金属产生一定的搅拌作用,从而促进了熔融金属的喷溅,并改善孔壁几何形貌和内壁质量。同时,旋转磁场会加速微孔出、入口处熔渣排出孔外,进一步改善了孔壁质量和微孔锥度,增加了刻蚀深度。目前大多研究将旋转磁场作为一种加工工艺进行简单对比,并未研究旋转磁场的转速对微孔形貌、喷溅、刻蚀深度和内壁氧含量的影响。本文在旋转磁场不同转速下,研究了微孔刻蚀深度、表面喷溅、孔壁几何形貌和内壁氧含量的变化,并探索了在有/无旋转磁场情况下,单脉冲能量对微孔锥度的影响。

2 试验装置及方法

2.1 试验设备

旋转磁场辅助激光加工系统示意图如图 1 所示,脉冲激光器发出的激光束经过反射镜后进入振镜系统,然后被聚焦透镜聚焦到材料上进行加工。其中,光源选用德国 EdgeWave 公司生产的 PX100-1-GM 型号 Nd:YAG 红外皮秒脉冲激光器(波长为 1064 nm,脉宽为 12 ps,光斑直径为 20 μm ,峰值输出功率为

收稿日期: 2021-07-05; 修回日期: 2021-09-04; 录用日期: 2021-11-12

基金项目: 国家自然科学基金(52075227, 51905226)、江苏省自然科学基金(BK20180873, BK20180875)、江苏大学工业中心大学生创新实践基金(ZXJG2021049)

通信作者: *zzhaoyang@126.com

70 W, 脉冲频率在 0.2~30 MHz 之间可调)。旋转磁场由三对 20 mm×15 mm×10 mm 钕铁硼磁铁组装而成, 磁铁被固定在特制圆盘夹具上, 由厚度为 9.6 mm 的超薄电机提供动力。磁铁为 N、S 极相斥放置, 相距 40 mm, 由 TD8620 手持式数字特斯拉计测得的中心磁场强度为 103 mT。静态磁场由一对相距 24 mm 且 N、S 极相对水平放置的钕铁硼磁铁组装而成, 经特斯拉计测量, 中心磁场强度为 103 mT。为了减小夹具对磁场的影响, 用尼龙材料 3D 打印制成特制圆盘, 放置样品的夹具由亚克力板粘连而成。试验装置图如图 2 所示。

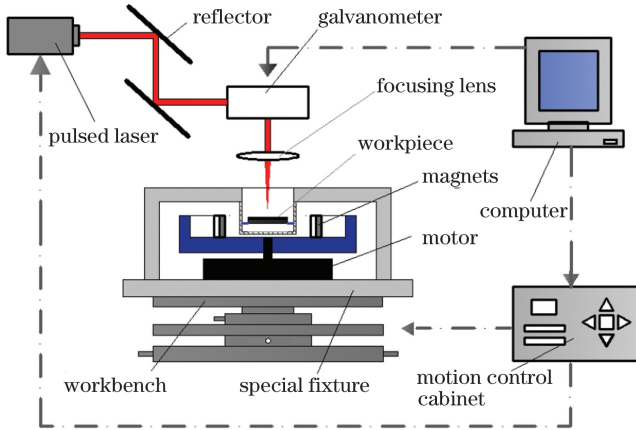


图 1 旋转磁场辅助激光加工系统示意图

Fig. 1 Schematic of magnetic field rotation assisted laser processing system

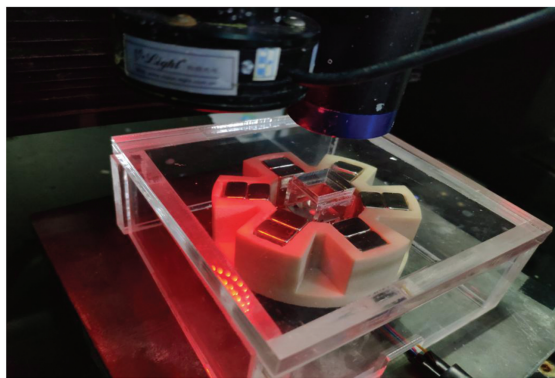


图 2 试验装置图

Fig. 2 Schematic of experimental setup

在试验过程中, 为了减小随机误差, 每个参数下均加工 5 个孔。加工好的微孔经超声清洗后, 利用激光器电荷耦合元件 (CCD) 进行测量, 测量方法如图 3(a) 所示, 对于每个孔, 每隔 60° 测量一次孔径, 分别测量微孔入口和出口孔径, 最后取其平均值。比较不同激光单脉冲能量作用下有/无旋转磁场对微孔锥度的影响。锥度计算示意图如图 3(b) 所示, 计算公式为

$$\theta = \arctan \left(\frac{D-d}{2H} \right), \quad (1)$$

式中: θ 为微孔锥度; D 为入口直径; d 为出口直径; H 为样品厚度。

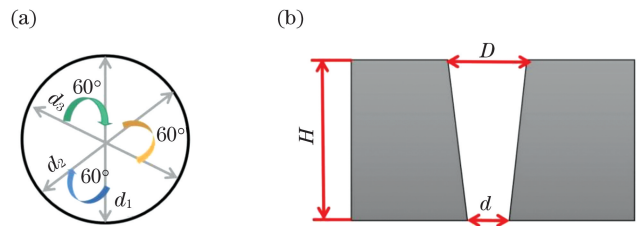


图 3 微孔孔径测量及锥度计算示意图。(a) 孔径测量; (b) 孔锥度计算

Fig. 3 Schematics of micro-hole diameter measurement and taper calculation. (a) Hole diameter measurement; (b) hole taper calculation

为了更清晰地观察到旋转磁场对微孔内壁几何形貌的影响并研究旋转磁场转速对微孔材料去除情况的影响, 利用钨灯丝扫描电子显微镜 (SEM) 观察微孔内壁和入口处的喷溅。为了观测旋转磁场对孔壁氧化物及熔融金属的影响, 对微孔进行能谱分析。为了研究有/无旋转磁场及旋转磁场不同转速对微孔刻蚀深度的影响, 分别对微孔加工 5 s 和 10 s 后, 利用超景深三维显微镜测量盲孔深度。

2.2 试验材料

样品为尺寸为 13.0 mm×19.0 mm×0.4 mm 的 304 不锈钢, 试验时被放置于专有夹具上。试验前, 对样品进行打磨、抛光, 并用无水乙醇进行超声清洗。分别用扫描电镜和激光器 CCD 相机观察微孔表面形貌并测量锥度。观察微孔内壁形貌时, 先用角磨机将加工好的样品打磨至接近微孔, 再用砂纸进行打磨并抛光, 超声清洗后利用扫描电镜观察。

3 试验结果与讨论

3.1 加工原理分析

激光直接加工的原理如图 4(a) 所示, 在激光钻孔过程中, 激光加工材料产生的等离子体对激光束具有屏蔽作用, 导致微孔质量变差 (如钻孔形貌质量差, 刻蚀深度小, 锥度大)。在激光直接刻蚀微孔过程中, 熔融材料产生的金属飞溅物会从微孔出、入口排出, 但有一部分材料因来不及排出孔口而冷凝附着在微孔出、入口附近, 导致微孔出、入口处形成熔渣残留。在微孔入口上方, 由于激光对空气的电离, 形成了大气等离子体, 激光焦点发生折射^[8]而下移, 从而微孔入口尺寸较大。

旋转磁场 (B) 辅助激光钻孔的机理如图 4(b) 所示, 其加工作用有以下几点。

1) 激光加工不锈钢材料产生的等离子体屏蔽了激光束能量, 使得微孔越往下加工能量的衰减越快。磁场对等离子体的约束作用会使等离子体沿磁场方向膨胀, 即在水平方向扩散, 从而减少对激光能量的削弱^[9]。故激光束能够更均匀地去除材料, 提升激光刻蚀深度。

2) 在微孔入口上方, 由于激光对空气的电离, 形成了大气等离子体^[10], 激光焦点发生折射而下移。旋转

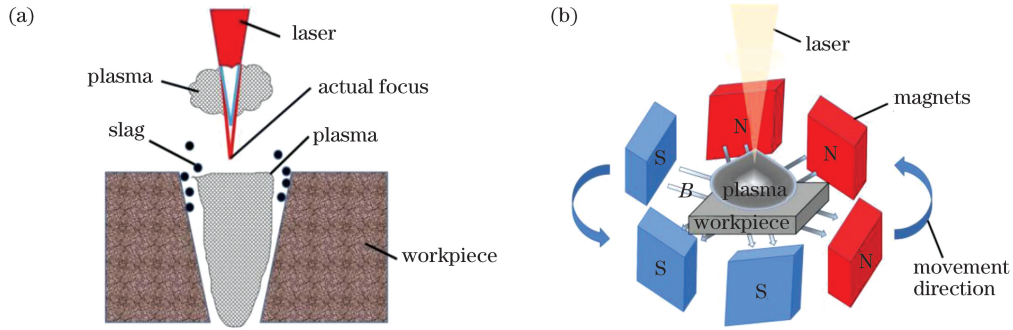


图 4 试验加工原理图。(a)激光直接加工;(b)旋转磁场辅助激光加工

Fig. 4 Schematics of experimental processing. (a) Laser direct processing; (b) magnetic field rotation assisted laser processing

磁场会进一步约束大气等离子体,减小激光焦点的偏移量,从而减小微孔入口直径,减小微孔锥度。

3) 旋转磁场会使激光熔池中的液体受到与旋转磁场方向一致的电磁力的作用,熔池中液体的对流加强,径向温度梯度减小^[11],从而内壁粗糙度进一步减小,内壁更加平整光滑,熔融物分布更加均匀。

4) 旋转磁场会加速等离子体中带电粒子的运动,促进熔融金属的搅拌,使得微孔出、入口处更多的熔渣和飞溅物排出微孔,从而提升微孔质量。

3.2 旋转磁场对微孔内壁几何形貌的影响

为了更清晰地观察到旋转磁场对微孔内壁几何形

貌的影响,对微孔内壁进行扫描电镜拍摄。所用激光频率(f)为 0.2 MHz,元素次数(n)为 120,扫描速度(v)为 300 mm/s,离焦量(z)为 0,单脉冲能量为 55 μ J。元素次数是指激光在每个元素上重复加工的次数。图 5 是激光直接加工、静态磁场辅助加工和旋转磁场辅助加工后的内壁截面图。对比图 5(a)、(b)可知,激光直接加工微孔时,内壁重铸层分布不均匀,沟壑明显。特别是微孔出、入口处,熔渣堆积较多。施加静态磁场后,孔壁重铸层和入口处的熔渣已有一定改善,但入口处仍然存在凹坑。这是因为磁场对激光加工材料产生的等离子体形成约束,致使其沿磁场方

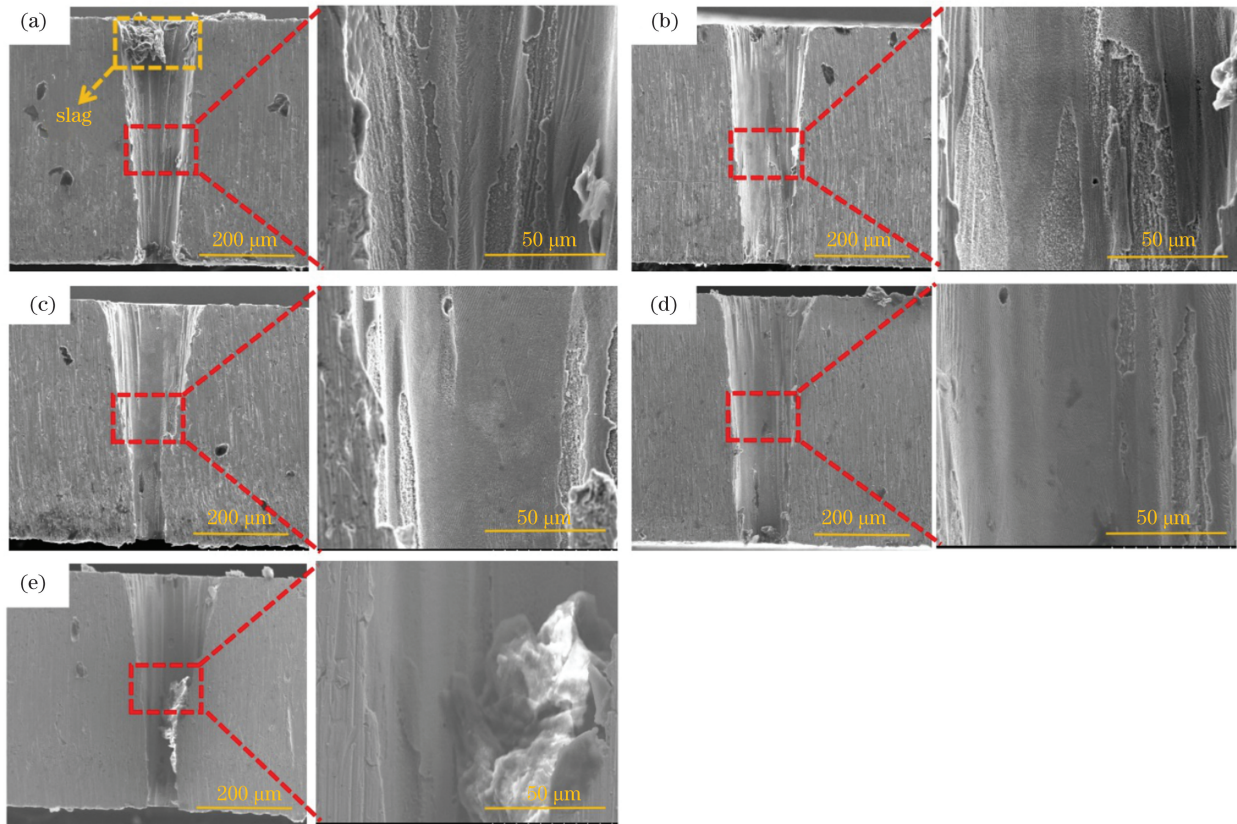


图 5 不同加工方式下的微孔内壁扫描电镜图。(a)激光直接加工;(b)静态磁场辅助加工;(c)旋转磁场(转速为 50 r/min)辅助加工;(d)旋转磁场(转速为 150 r/min)辅助加工;(e)旋转磁场(转速为 250 r/min)辅助加工

Fig. 5 SEM images of micro-hole inner walls under different processing methods. (a) Laser direct processing; (b) static magnetic field assisted processing; (c) magnetic field rotation (speed of 50 r/min) assisted processing; (d) magnetic field rotation (speed of 150 r/min) assisted processing; (e) magnetic field rotation (speed of 250 r/min) assisted processing

向膨胀,从而减小了对激光的屏蔽作用,所以激光能够更好去除材料。对比图 5(b)、(c)可知,施加旋转磁场后,孔壁熔融物分布更加均匀,通孔去除均匀性得到进一步改善。同时,微孔出、入口处的熔渣残留较少。这是因为施加旋转磁场后,由旋转磁场产生的洛伦兹力使得等离子体中的带电粒子作加速运动,这对熔融金属有一定搅拌作用,从而对孔壁形成二次加工;同时,旋转磁场会加速微孔出、入口处熔渣排出孔外,有利于改善孔壁几何形貌和提高内壁质量。

对比图 5(c)、(d)、(e)可知,随着旋转磁场转速的增加,孔壁变得更加光滑,熔渣及内壁沟壑显著增多。猜测是旋转磁场转速过大,引起加工平台振动,使得加工不稳定。

3.3 旋转磁场对表面喷溅的影响

为了研究旋转磁场转速对微孔材料去除情况的影响,利用扫描电镜拍摄微孔入口处的喷溅。所用激光频率为 0.2 MHz,元素次数为 120,扫描速度为 300 mm/s,离焦量为 0,单脉冲能量为 55 μJ 。图 6(a)~(d)为激光直接加工和不同转速旋转磁场辅助加工的微孔入口处的表面喷溅图。由图 6(a)可知,在激光直接加工时,入口处表面喷溅较少。由图 6(b)、(c)、(d)知,当施加旋转磁场辅助加工时,表面飞溅物增多,且随着旋转磁场转速的增加,表面飞溅物的增加更为明显。这是由于旋转磁场的引入加速了内壁熔融金属的搅拌,入口处更多的熔渣和飞溅物排出微孔,说明微孔去除量增加,内壁更加平整光滑。

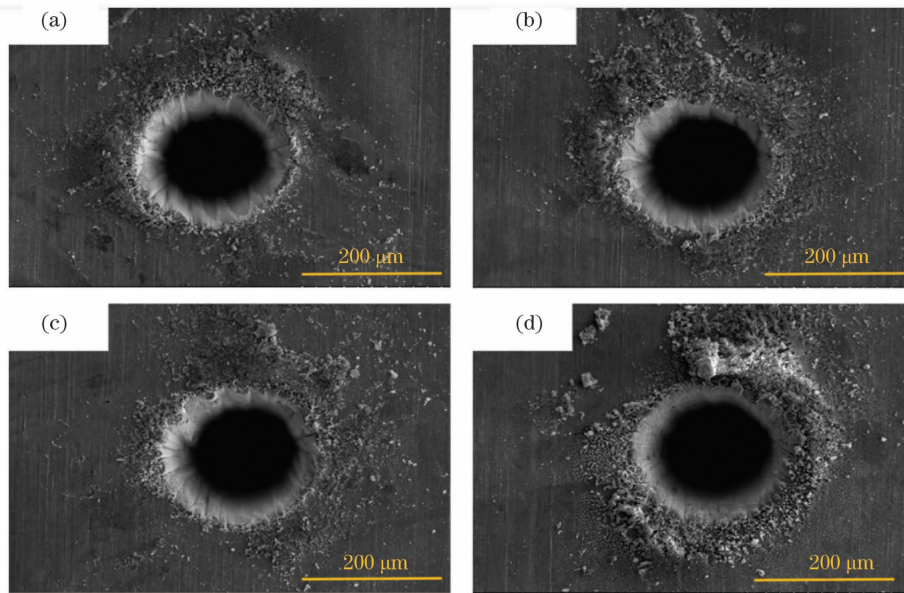


图 6 不同加工方式下微孔入口处的喷溅扫描电镜图。(a)激光直接加工;(b)旋转磁场(转速为 50 r/min)辅助加工;(c)旋转磁场(转速为 150 r/min)辅助加工;(d)旋转磁场(转速为 250 r/min)辅助加工

Fig. 6 SEM images of splashing at micro-hole entrance under different processing methods. (a) Laser direct processing; (b) magnetic field rotation (speed of 50 r/min) assisted processing; (c) magnetic field rotation (speed of 150 r/min) assisted processing; (d) magnetic field rotation (speed of 250 r/min) assisted processing

3.4 旋转磁场对微孔内壁氧含量的影响

为了研究旋转磁场对孔壁氧化物及熔融金属的影响,对微孔进行能谱分析,分别对微孔进行区域扫描(图 7)和线扫描(表 1)。由图 7 可知,在不施加磁场时,内壁氧含量(质量分数)为 24.8%,施加旋转磁场后氧含量降低。且随着旋转磁场转速由 50 r/min 到 150 r/min 再到 250 r/min 的增加,内壁氧含量逐渐减小,由 16.56% 减少到 8.05% 再到 7.83%。对内壁截面进行线扫描,同样可得此结论。如表 1 所示,在不施加磁场时,内壁氧含量为 12.76%,而在旋转磁场辅助下,内壁氧含量进一步降低。在转速为 50 r/min 时氧含量为 6.94%,转速为 150 r/min 时氧含量为 6.32%,转速为 250 r/min 时氧含量为 5.95%。这是由于旋转磁场的引入加速了内壁熔融金属的流动,内壁重铸层形貌更加光滑,同时旋转磁场也加速了微孔

出、入口处熔渣的排出。氧含量反映出内壁熔渣的残余,施加旋转磁场后,微孔内熔渣减少,且随着转速的增加,孔内排出的熔渣增多。

3.5 旋转磁场对微孔刻蚀深度的影响

为了研究有/无旋转磁场及旋转磁场转速对微孔刻蚀深度的影响,分别对加工 5 s 和 10 s 时的盲孔深度进行超景深三维显微测量。所用激光频率为 1.5 MHz,元素次数为 120,扫描速度为 300 mm/s,离焦量为 0,单脉冲能量为 5.87 μJ 。由图 8~10 可知,施加旋转磁场后微孔刻蚀深度增加,且随着旋转磁场转速的增加,微孔刻蚀深度也增加。这是由于激光加工不锈钢材料时产生的等离子体屏蔽了激光束的能量,微孔越往下加工能量衰减越快。而旋转磁场对等离子体具有约束作用,致使等离子体沿磁场方向膨胀,即在水平方向扩散,从而减少对激光能量的削

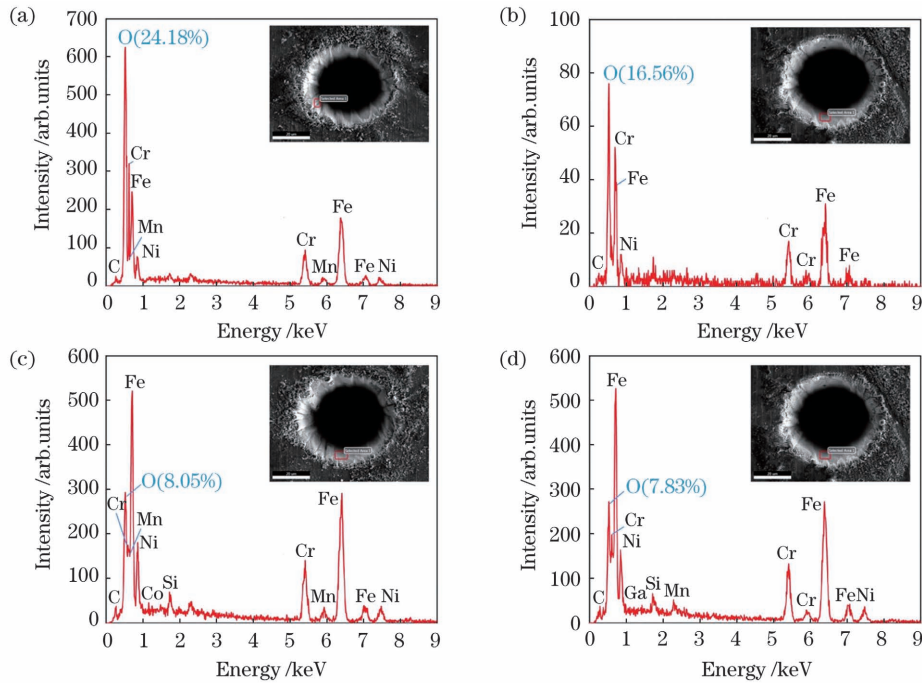


图 7 不同加工方式下微孔内壁的能谱图。(a)激光直接加工;(b)旋转磁场(转速为 50 r/min)辅助加工;(c)旋转磁场(转速为 150 r/min)辅助加工;(d)旋转磁场(转速为 250 r/min)辅助加工

Fig. 7 Energy spectra of micro-hole inner walls under different processing methods. (a) Laser direct processing; (b) magnetic field rotation (speed of 50 r/min) assisted processing; (c) magnetic field rotation (speed of 150 r/min) assisted processing; (d) magnetic field rotation (speed of 250 r/min) assisted processing

表 1 内壁线扫描测得的氧元素含量

Table 1 Oxygen element content measured by line scan of inner wall

Magnetic field	Mass fraction of oxygen element %
No magnetic field	12.76
Rotating magnetic field with speed of 50 r/min	6.94
Rotating magnetic field with speed of 150 r/min	6.32
Rotating magnetic field with speed of 250 r/min	5.95

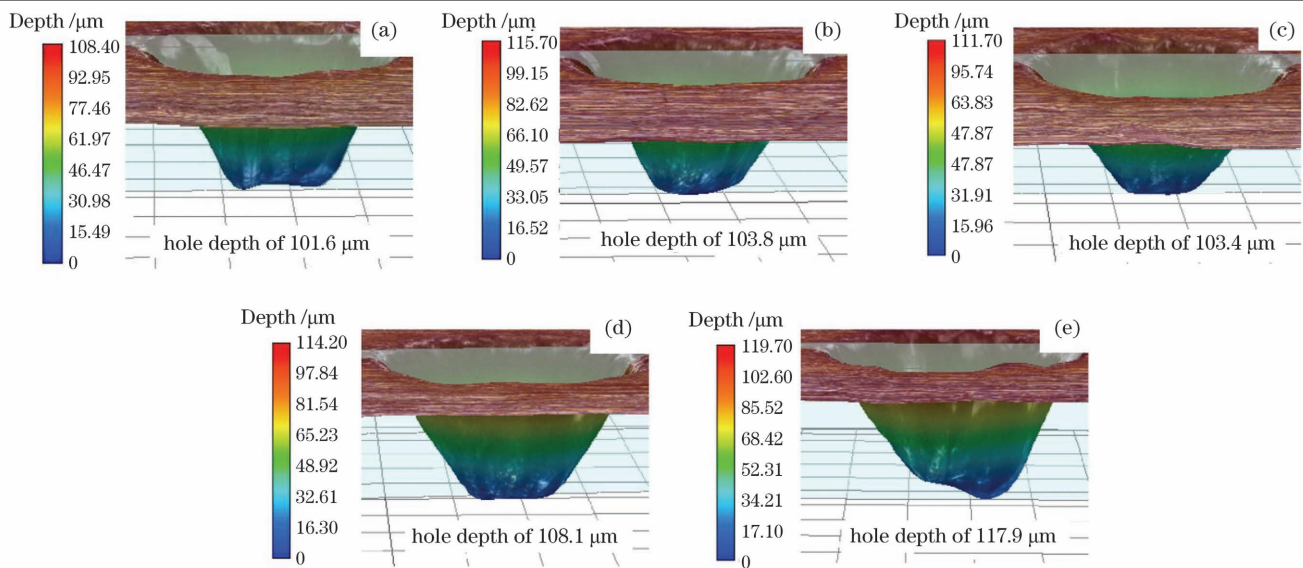


图 8 微孔加工 5 s 后的超景深显微镜图。(a)激光直接加工;(b)旋转磁场(转速为 50 r/min)辅助加工;(c)旋转磁场(转速为 150 r/min)辅助加工;(d)旋转磁场(转速为 250 r/min)辅助加工;(e)旋转磁场(转速为 350 r/min)辅助加工

Fig. 8 Ultra-depth-of-field microscope images of micro-hole after processing for 5 s. (a) Laser direct processing; (b) magnetic field rotation (speed of 50 r/min) assisted processing; (c) magnetic field rotation (speed of 150 r/min) assisted processing; (d) magnetic field rotation (speed of 250 r/min) assisted processing; (e) magnetic field rotation (speed of 350 r/min) assisted processing

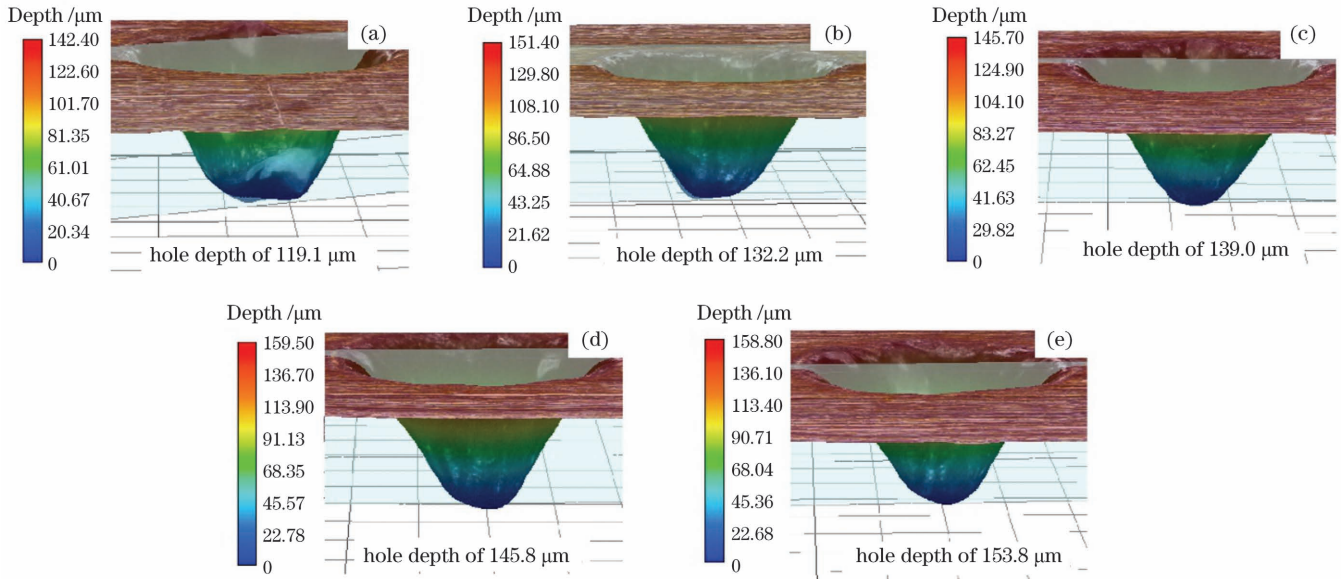


图 9 微孔加工 10 s 后的超景深显微镜图。(a)激光直接加工;(b)旋转磁场(转速为 50 r/min)辅助加工;(c)旋转磁场(转速为 150 r/min)辅助加工;(d)旋转磁场(转速为 250 r/min)辅助加工;(e)旋转磁场(转速为 350 r/min)辅助加工

Fig. 9 Ultra-depth-of-field microscope images of micro-hole after processing for 10 s. (a) Laser direct processing; (b) magnetic field rotation (speed of 50 r/min) assisted processing; (c) magnetic field rotation (speed of 150 r/min) assisted processing; (d) magnetic field rotation (speed of 250 r/min) assisted processing; (e) magnetic field rotation (speed of 350 r/min) assisted processing

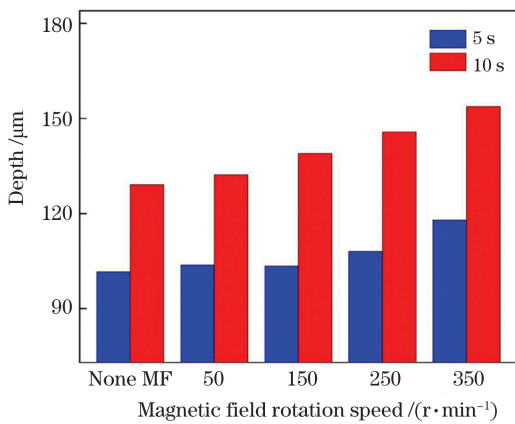


图 10 不同加工时间下微孔刻蚀深度随磁场转速的变化
Fig. 10 Micro-hole etching depth versus magnetic field rotation speed under different processing time

弱。故施加旋转磁场后,激光束能够更均匀地去除材料,激光刻蚀深度增加。且随着旋转磁场转速的增加,更多的孔内熔渣和飞溅物排出孔外,同时旋转磁场能够更加均匀地对刻蚀产生的等离子体施以约束,从而微孔刻蚀深度随旋转磁场转速的增加而增加。由图 10 可知,当旋转磁场转速为 350 r/min 且加工时间为 10 s 时,相较前一转速,刻蚀深度增加量达到最大,为 24.7 μm 。

3.6 不同单脉冲能量下有/无旋转磁场对微孔锥度的影响

对尺寸为 13.0 mm×19.0 mm×0.4 mm 的 304 不锈钢分别进行激光直接打孔和旋转磁场辅助激光打孔(旋转磁场转速为 50 r/min),从而比较不同单脉冲

能量作用下有/无旋转磁场对微孔锥度的影响。所用激光频率为 0.2 MHz,元素次数为 120,扫描速度为 300 mm/s,离焦量为 0,单脉冲能量为 25~85 μJ 。

图 11 对比了有/无旋转磁场时的微孔出入口及内壁锥度。随着单脉冲能量的增大,施加旋转磁场后微孔锥度的减小更明显。当单脉冲能量变大时,旋转磁场下微孔入口直径减小得更多,出口直径略有增加,故较大能量时微孔锥度的减小明显。

如图 12 所示,随着激光单脉冲能量的增加,旋转磁场辅助下的微孔入口直径小于激光干刻,微孔出口直径始终大于激光干刻。在单脉冲能量为 25 μJ 时,两种工艺下微孔出、入口孔径值差距较小,随着单脉冲能量的增加,两种加工工艺下对应的微孔孔径差值增大。在单脉冲能量为 25 μJ 时,两种加工工艺下的微孔锥度几乎一致。随着单脉冲能量的增加,旋转磁场辅助下的微孔锥度逐渐减小,两种工艺下的锥度差值越来越显著。在单脉冲能量为 85 μJ 时,两种工艺下的微孔锥度差值最大,旋转磁场辅助下的微孔锥度比激光干刻的锥度小 1.17°。这是因为激光加工过程中产生的气态物质和等离子体云阻碍了激光的传播,所以激光能量随孔深的增加而减小。而旋转磁场的引入加速了等离子体的扩散作用,削弱了等离子体对脉冲激光的屏蔽作用。单脉冲能量越大,激光与材料作用产生的等离子体越密集,磁场的约束作用越显著,因此等离子体越蓬松,此时激光束能够更好穿透材料,故单脉冲能量为 85 μJ 时两种工艺下的锥度差值最大。

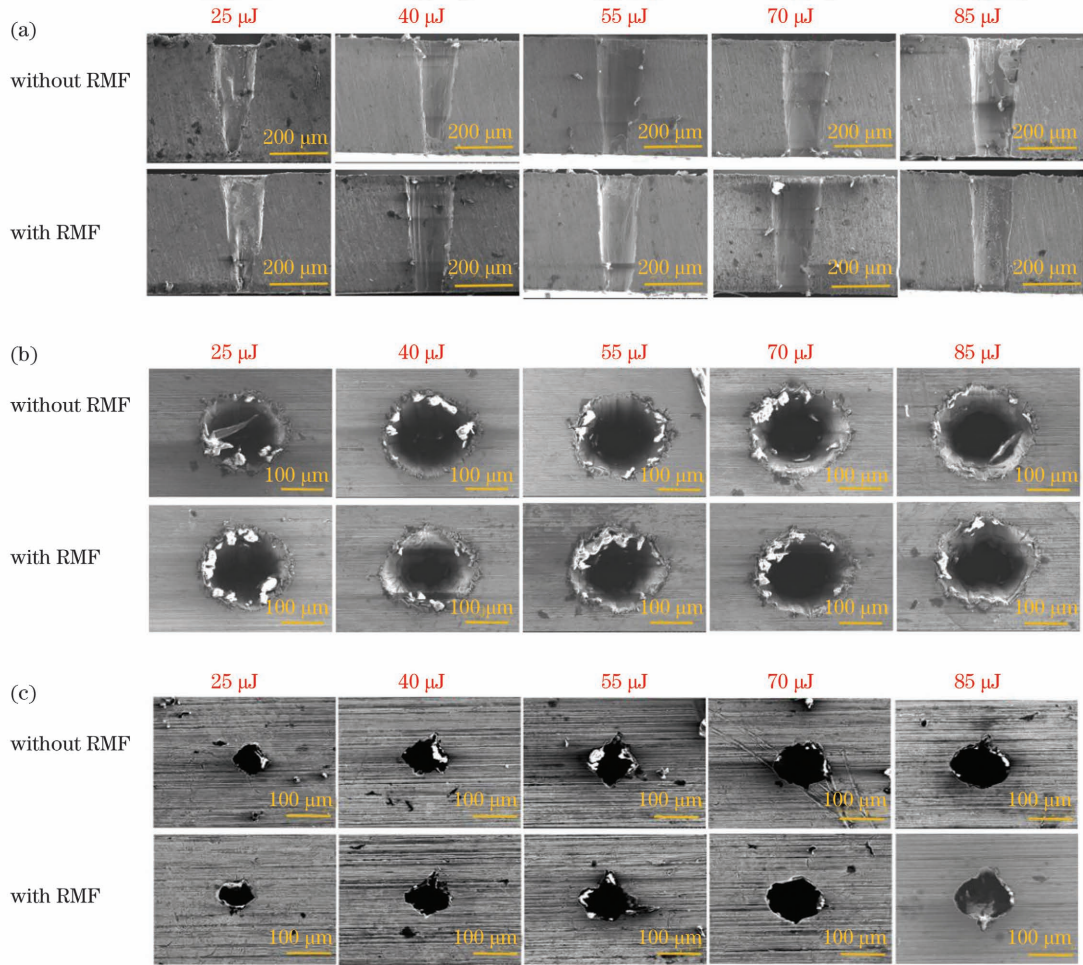


图 11 不同单脉冲能量下的微孔截面和出、入口电镜图。(a)微孔截面;(b)微孔入口;(c)微孔出口
Fig. 11 SEM images of micro-hole cross-sections, inlets and outlets under different single pulse energies. (a) Micro-hole cross-section; (b) micro-hole inlet; (c) micro-hole outlet

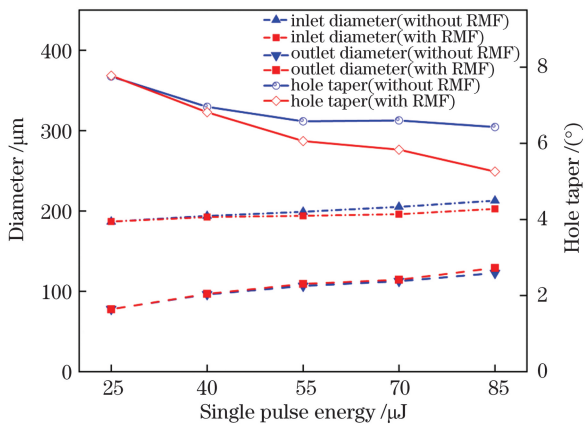


图 12 不同加工工艺下的微孔锥度对比图
Fig. 12 Comparison of micro-hole tapers under different processing techniques

4 结 论

采用对比试验的方法,研究了在旋转磁场不同转速下,微孔刻蚀深度、表面喷溅、孔壁几何形貌和氧含量的变化,并探索了在有/无旋转磁场情况下,单脉冲能量对微孔锥度的影响。

1) 旋转磁场辅助激光加工可以改善微孔内壁形貌,减少出、入口处的熔渣,使内壁重铸层分布更均匀,孔壁更加光滑。旋转磁场具有搅拌作用,可以加速微孔出、入口处的熔渣飞溅,致使内壁氧含量降低。且随着旋转磁场转速的增加,内壁氧含量逐渐减少,但过快的转速会使得孔壁几何形貌逐渐变差,内壁熔渣和沟壑显著增多。

2) 通过施加旋转磁场,微孔表面喷溅更为显著。且随着旋转磁场转速的增加,喷溅量逐渐增大,故旋转磁场可以加速内壁熔融金属的喷溅,提高内壁加工质量。

3) 旋转磁场能够对激光加工材料产生的等离子体进行更均匀的约束,提升激光刻蚀深度。在旋转磁场转速为 350 r/min 且加工时间为 10 s 时,刻蚀深度的增加量达到最大,为 24.7 μm。

4) 单脉冲能量越大,激光与不锈钢材料作用产生的等离子体越密集,磁场的约束作用越显著,微孔锥度减小得越明显。在激光单脉冲能量为 85 μJ 时,两种工艺下的微孔锥度差值最大,旋转磁场辅助下的微孔锥度比激光干刻下的锥度小 1.17°。

参 考 文 献

- [1] Lus Y, Sun G F, Wen D P, et al. Effects of applying electric and magnetic fields on laser drilling [J]. The International Journal of Advanced Manufacturing Technology, 2016, 84(9/10/11/12): 2293-2300.
- [2] Chang Y J, Kuo C L, Wang N Y. Magnetic assisted laser micromachining for highly reflective metals[J]. Journal of Laser Micro/Nanoengineering, 2012, 7(3): 254-259.
- [3] 朱苏凯. 有/无磁场条件下水基超声振动辅助激光打孔的机理研究[D]. 镇江: 江苏大学, 2019: 61-77.
Zhu S K. Investigation on mechanisms for water-based ultrasonic vibration-assisted laser drilling with/without magnetic filed[D]. Zhenjiang: Jiangsu University, 2019: 61-77.
- [4] Ye C, Cheng G J, Tao S, et al. Magnetic field effects on laser drilling[J]. Journal of Manufacturing Science and Engineering, 2013, 135(6): 061020.
- [5] Balamurugan S, Manikandan C B, Balamurugan P. A study on magnetic field assisted laser percussion drilling and its effect on surface integrity [J]. Archives of Materials Science and Engineering, 2018, 94(1): 35-40.
- [6] 李涛. 磁场辅助脉冲激光旋切制孔机理研究[D]. 镇江: 江苏大学, 2020: 72-79.
Li T. Investigation on mechanism analysis for pulsed laser hole-trepanning using magnetic assistance [D]. Zhenjiang: Jiangsu University, 2020: 72-79.
- [7] Patwari A U, Noor S, Chowdhury M S I, et al. Effect of external magnetic field on drilled hole quality during drilling operation[C]// International Conference on Mechanical, Industrial and Materials Engineering, November 1-3, 2013, RUET, Rajshahi, Bangladesh. RUET: ICMIME, 2013, 28: 498-502.
- [8] Wang H X, Zhu S K, Xu Y, et al. Experimental investigation on effects of water-based ultrasonic vibrations, transverse magnetic field and water temperatures on percussion laser drilling performance [J]. Optics & Laser Technology, 2019, 112: 395-408.
- [9] Wolff S, Saxena I. A preliminary study on the effect of external magnetic fields on Laser-Induced Plasma Micromachining (LIPMM)[J]. Manufacturing Letters, 2014, 2(2): 54-59.
- [10] 赵万芹, 梅雪松, 王文君. 超短脉冲激光微孔加工(上): 理论研究[J]. 红外与激光工程, 2019, 48(1): 0106008.
Zhao W Q, Mei X S, Wang W J. Ultrashort pulse laser drilling of micro-holes(part 1): theoretical study[J]. Infrared and Laser Engineering, 2019, 48(1): 0106008.
- [11] 王维, 刘奇, 杨光, 等. 电磁搅拌辅助钛合金激光沉积修复的电磁场模拟与验证[J]. 红外与激光工程, 2015, 44(9): 2666-2671.
Wang W, Liu Q, Yang G, et al. Numerical simulation and verification of electromagnetic field in titanium alloy laser deposition repair with electromagnetic stirring[J]. Infrared and Laser Engineering, 2015, 44(9): 2666-2671.

Mechanism and Experimental Research of Magnetic Field Rotation Assisted Laser Machining of Micro-Holes

Wang Yinfei, Zhu Hao, Zhang Zhaoyang*, Zhang Tianshuai, Wu Yucheng, Du Wenwu
School of Mechanical Engineering, Jiangsu University, Zhenjiang 212013, Jiangsu, China

Abstract

Objective With the advancement of science and technology in the aerospace sector, the micro-hole laser processing tools have become increasingly important. Compared to traditional machining and electric spark processing of micro-plates, laser drilling has high processing efficiency, high speed, low cost, and wide application range, and a lot of high sensitive holes can be processed. An ultrashort laser pulse has gradually become the preferred one for high-quality micro-hole processing due to its high processing accuracy, but the existing studies have found that an ultrashort pulse laser still has defects such as recast layers, micro-cracks, and slags, and at the same time, the processing efficiency is far less than that for a traditional long laser pulse. Magnetic field assisted laser drilling can further reduce the defects of ultrashort laser processing to improve the micro-hole morphology, increase the etching depth, and reduce the hole taper. In order to further improve the geometry for laser drilling, improve the etching depth, and reduce the hole taper, the 304 stainless steel is used as the test material and the magnetic field rotation assisted laser drilling and machining is adopted.

Methods This paper discusses the mechanism and experimental study of magnetic field rotation assisted laser drilling of 304 stainless steel. First, the effect of magnetic field rotation on the quality of microporous processing is studied. The variations of micro-hole etching depth, the surface spatter, the hole-wall geometry, and the oxygen content of inner wall are investigated under the action of different magnetic field rotation speeds. The microporous surface splatter and the inner-wall morphology are observed by the scanning electron microscope. The inner-wall removal amount is described with surface splatter, and the inner-wall quality is described with inner wall smooth flatness. Then, the inner-wall oxygen content is measured by the energy spectrometer, and it can reflect the inner-wall slag and the recast layer of the micro-holes. The inner-wall regional scanning and line scanning are studied at different magnetic field rotation speeds, which can infer the variation of inner-wall oxygen content (inner-wall slag and recast layer) with magnetic field rotation. The micro-hole etching depth is measured by the ultra-depth-of-field microscope, the micro-hole etching depth is quantified, and the etching depths under different rotation speeds for 5 s and 10 s are compared. Finally, the effect of magnetic field rotation on the micro-hole taper is studied under different single pulse energies. It can be evaluated from the micro-hole

inlet size, outlet size, and inner-wall taper.

Results and Discussions After applying a rotating magnetic field, the Lorenz force generated by the rotating magnetic field accelerates the motion of the charged particles in plasma and simultaneously the molten metal has a certain agitation and splash, so the inner-wall melt distribution is more uniform and the removal uniformity of the through-hole is further improved (Fig. 5). When the rotating magnetic field is applied, the surface splash is increased. The surface splatter is increased more significantly as the magnetic field rotation speed is increased to 250 r/min (Fig. 6). The application of the rotating magnetic field can accelerate the flow of the inner-wall molten metal. Therefore the inner-wall morphologies of the recast layers are smoother, and it can also accelerate the discharge of the slags in the micro-hole inlet and outlet. The oxygen content reflects the residues of inner-wall slags, indicating that the micro-hole slags are reduced after applying a rotating magnetic field (Fig. 7). As the magnetic field rotation speed increases, the micro-hole etching depth also increases. When the magnetic field rotation speed is 350 r/min and the processing time is 10 s, the increase of etching depth reaches the maximum of 24.7 μm (Figs. 8, 9, and 10). Compared those with and without a rotating magnetic field when the single pulse energy becomes large, the diameter of the micro-hole inlet under the rotating magnetic field is significantly reduced and the outlet diameter is slightly increased, so the micro-hole taper is reduced more significantly under a larger energy. When the single pulse energy of the laser is 85 μJ , the micro-hole taper difference between the two processes is the largest, and the micro-hole taper under a rotating magnetic field is reduced by 1.17° compared with that by laser direct processing (Figs. 11 and 12).

Conclusions The variations of micro-hole etching depth, the surface spatter, the hole-wall geometry, and the inner-wall oxygen content are investigated under the action of magnetic fields with different rotation speeds. The effect of single pulse energy on the micro-hole taper is studied with and without the action of a rotating magnetic field. Experiments show that with the increase of magnetic field rotation speed, the micro-hole etching depth increases, the surface splashing becomes more pronounced, and the oxygen content further decreases. The introduction of a rotating magnetic field makes the geometric shape of the hole-wall smooth and can effectively reduce the micro-hole taper. The higher the energy of a single pulse, the more significant the decrease in micro-hole taper.

Key words laser technique; laser drilling; rotating magnetic field; morphology; taper; etching depth